Effects of Nonlinearities on the Steady State Dynamic Behavior of Electric Actuated Microcantilever-based Resonators

R.N. Jazar, M. Mahinfalah, N. Mahmoudian and M.A. Rastgaar

Journal of Vibration and Control 2009 15: 1283 originally published online 6 July 2009
DOI: 10.1177/1077546307086443

Effects of Nonlinearities on the Steady State Dynamic Behavior of Electric Actuated Microcantilever-based Resonators

R. N. JAZAR
Department of Mechanical Engineering, Manhattan College, Riverdale, NY 10471, USA (Reza.Jazar@manhattan.edu)

M. MAHINFALAH
Department of Mechanical Engineering, Milwaukee School of Engineering, Milwaukee, WI 53202, USA

N. MAHMOUDIAN
Nonlinear Systems Laboratory (NSL), Department of Aerospace and Ocean Engineering, Virginia Polytechnic Institute and State University, Blacksburg, VA 24061, USA

M. A. RASTGAAR
Center for Vehicle Systems and Safety (CVeSS), Virginia Polytechnic Institute and State University, Blacksburg, VA 24060, USA

(Received 24 May 2005; accepted 10 October 2007)

Abstract: This paper presents the dynamic behavior of microcantilever-based microresonators and compares their steady state behavior for polarized and nonpolarized systems at different levels of nonlinearities. A microcantilever, equipped with a time-varying capacitor, makes the microresonator system. The capacitor is activated by a constant polarization voltage, and an alternative actuating voltage. The partial differential equation of motion of the vibrating electrode can be reduced to a highly nonlinear parametric second order ordinary differential equation. The steady state behavior of the microresonator has been analyzed with and without polarization voltage. The main characteristic of the non-polarized model is explained by the stability of the system in parameter plane. A set of stability chart is provided to predict the boundary between the stable and unstable domains. Furthermore, the main characteristic of the polarized model is determination by the period-amplitude relationship of the system. Applying perturbation methods, analytical equations are derived to describe the frequency response of the system, which are suitable to be utilized in parameter study and design.

Key words: MEMS, microresonator, acceleration sensors, parametric resonance, stability diagram, nonlinear Mathieu equation.

Journal of Vibration and Control, **15(9):** 1283–1306, 2009 DOI: 10.1177/1077546307086443

Figures 1, 5–15 appear in color online: http://jvc.sagepub.com

NOTATION

A	Effective area of plate
c	Equivalent viscous damping rate
d	Gap size
f	Electrostatic force
F	Dimensionless electrostatic force
g	Function
$h = c/\sqrt{k_1 m}$	Dimensionless damping rate
J	Jacobian matrix
$k = k_1 + k_2 x^2$	Equivalent spring rate
l	Linear dimension
m	Mass
O	Order of magnitude symbol
$r = \omega/\omega_n$	Dimensionless excitation frequency
$\mathbf{R}$	Real numbers set
S	Stable symbol
t	Time
U	Unstable symbol
$v = v_i \sin(\omega t)$	Alternative voltage
v_i	Amplitude of alternative voltage
v_p	Polarization voltage
x	Longitudinal coordinate
y	Lateral coordinate; Displacement of plate
y_s	Equilibrium point
Y	Dimensionless amplitude of oscillations
Z	Short note symbol
$\alpha = \varepsilon_0 A v_P^2 / \left(2k_1 d^3\right)$	Polarization voltage parameter
$\beta = \varepsilon_0 A v_i^2 / \left(4k_1 d^3\right)$	Alternative voltage parameter
β_1, β_2	Transition curves
$\lambda = k_2 d^2 / k_1$	Nonlinear spring parameter
ε_0	Permittivity in vacuum
$\tau = \omega_n t$	Dimensionless time
ω	Frequency of alternative voltage
$\omega_n = \sqrt{k_1/m}$	Natural frequency of linearized model
∂	Derivative
$(\,)'$	$d(\,)/d\tau$
overdot	$d(\,)/dt$

1. INTRODUCTION

Micro-electro-mechanical systems (MEMS) are microscopic mechanical systems coupled with electric circuits. Microcantilever-based MEMS have been extensively used as micro-scale high-quality oscillators in communication resonators, microphones, amplifiers, micro-sensors, micro-actuators, micro-engines, micro-instruments, micro-optics, micro-fluidics and

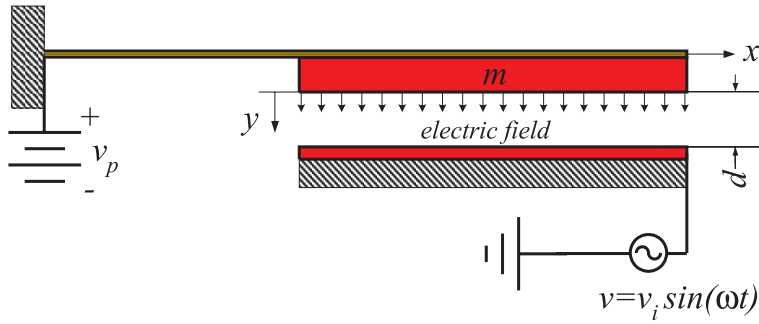

Figure 1. A simplified time-varying mechanical model of the MEMS.

other micro-oscillatory devices. MEMS generally have three components: an input transducer, a mechanical resonator and an output transducer. The input transducer converts an input electrical signal into a mechanical force. The mechanical resonator magnifies the input signal; and finally, the output transducer senses the motion of the mechanical resonator and generates a corresponding electrical signal (Raskin et al., 2000).

Mathematical model of microresonators usually indicate a nonlinear parametric system. So, the stability of the system depends on the value of its parameters. The output signal of MEMS is not reliable when it is operating in a saturated or in an unstable region. From a design viewpoint, a stability chart is needed to indicate the relationship between the parameters to determine if the system is stable, periodic, or unstable.

Most MEMS devices are modeled using weak analytical tools, resulting in a relatively inaccurate prediction of performance behavior. As a result, the MEMS design process is usually performed in a trial-and-error fashion, requiring several iterations before the performance requirements of a given device are finally satisfied. Having suitable design tools, combined with computer networks, can radically alter this situation (Sigmund, 2001; Younis, Abdel-Rahman, and Nayfeh, 2003; Younis, 2004).

The microresonator, which is studied in this investigation, is an electrostatically actuated microcantilever. Microcantilevers have a wide range of applications, because of simple geometry, easy production, durability, and compact area of motion. As a few examples: force and motion detectors, mechanical filters for telecommunications and chemical sensor arrays are the most common applications that use microcantilevers. Microresonators are also extensively utilized for acceleration sensors, inertial navigation units, electromechanical signal processing, microengines, weapons fusing and mass-storage devices (Younis 2004; Nayfeh and Younis, 2004).

In this paper, we model and analyze a microcantilever-based resonator (shown in Figure 1) from an Eulerian view point. More specifically, we examine the system in a coordinate system attached to the tip of the microcantilever at the static equilibrium position. Because of nonlinearities, the system has multiple equilibria. The positions of the equilibria are functions of the polarization voltage, and therefore they are not fixed globally. However, they can be fixed in a proper coordinate frame. The new method of modeling introduces several advantages. Among them are: the more sensible position of equilibria, a simpler bifurcation plot, and a simpler analytic description of the frequency response of the system.

The electrostatic force nonlinearly depends on the gap size between the two electrodes. When one of the electrodes is moving, the force would be nonlinear and time depended. Hence, the governing equation of motion of the MEMS is a highly nonlinear parametric equation. Such a system needs to have a stability chart to operate in a stable region with a safe margin (Younis and Nayfeh, 2003).

Using perturbation methods, the stability and steady state amplitude-period dependency of the MEMS will be studied extensively to indicate the boundaries of stable and unstable regions in parametric space. We examine the steady state dynamic behavior of the system affected by varying parameters and the level of nonlinearity. The purposes of this investigation are: first, to study the dynamic of microbeam resonators at steady state condition, and second, to indicate that for a highly nonlinear electric actuated microresonators, simplification of the nonlinearities will generate results which are far from the actual response of the system. Therefore, a full nonlinear analysis is needed to predict and design the dynamic behavior of the system.

A nondimensionalized mathematical model of the resonator is utilized to provide the dynamic properties of the system. The system is analyzed in two categories: with polarization, and without polarization. In each category we start with investigating the linearized model of the system. Then by increasing the effect of amplitude, different nonlinear models will be examined. In the case of no polarization voltage, no frequency response can be detected for the linearized model, and therefore a stability analysis of the system must be done to provide a stability diagram. Provided that a stability diagram can be found, it is possible to design the parameters to keep the system in a stable condition. The system shows a frequency response when a polarization voltage is introduced. Using perturbation method, analytical equations will be developed to describe the frequency responses.

Despite the substantial progress made in computer-based geometrical study of nonlinear dynamic systems, there is still a useful role to be played by approximate analytical techniques such as the averaging or multiple scale methods. The versatility of closed form solutions greatly assists the design engineering purposes. Furthermore, these approximate analytic results can often be utilized as a guide to locate areas of particular interest before conducting a more thorough and comprehensive analysis (Jazar and Golnaraghi, 2002).

2. MATHEMATICAL MODELING AND COLLAPSE LOAD

Consider the model of an electrically actuated microcantilever resonator with a variable capacitor as shown in Figure 1. The fixed plate of the capacitor, with an effective area A, is connected to an alternating current voltage $v = v_i \sin(\omega t)$ where v_i, and ω, are the AC amplitude and frequency, respectively. The other plate of the capacitor is a movable rigid microplate with an effective mass m. The supporting beam of the moving plate is simplified as a nonlinear spring with a stiffness $k(Y)$, parallel to a linear damper of damping h, where Y is the deflection of the microbeam at the tip. The moving plate, might be connected to a polarization voltage v_p.

The clearance between the two plates of the capacitor is d, which is measured when the polarization voltage and excitation frequency are zero. Such a system obeys a partial differential equation, however applying a separation of variables, $y = S(x) \cdot y(t)$, and

accepting the first harmonic mode shape for the spatial function reduces the equation of motion to an ordinary differential equation for temporal function $y(t)$. This kind of reduction of the equation of motion has been used and applied successfully (Jazar, 2006).

The coordinate for measuring the displacement of the moving plate is y, and if the location of its origin is at the position of the moveable plate when $v_p = v = 0$, then the simplest reduced-order equation of motion for the microbeam resonator is

$$m\ddot{y} + c\dot{y} + ky = F \quad \dot{y} = \frac{dy}{dt} \tag{1}$$

$$F = \frac{\varepsilon_0 A \left(v - v_p\right)^2}{2\left(d - y\right)^2} = \frac{\varepsilon_0 A}{2\left(d - y\right)^2}\left[v_P^2 + \frac{1}{2}v_i^2 + 2v_P v_i \sin\left(\omega t\right) - \frac{1}{2}v_i^2 \cos\left(2\omega t\right)\right] \tag{2}$$

where, ε_0 is permittivity in vacuum, and the electric force F is (Hsu, 2002).

The equivalent mass of the rigid microplate is $m = m_p + 0.2267m_b$, including the mass of the plate m_p and equivalent mass of the beam $0.2267m_b$. Damping strongly affects the dynamics, control, and performance of the system. There are several energy dissipation mechanisms in microresonator devices. Air-damping, squeezed-film damping, crystallographic defects, thermoelastic damping, internal, structural, intrinsic losses, and clamping losses are the most common sources of energy dissipations (Nguyen, 1995; Younis and Nayfeh, 2003; Wang et al., 2000; Jazar, 2006). Mostly, damping and dissipation mechanisms are mixed and coupled; however it is conventional to define an equivalent viscous damping for most of them (Wang et al., 2000). Among them, the squeezed-film damping and thermal damping are the most important and unavoidable ones. Stiffness of the microcantilever is also another important parameter that can be affected by thermoelastic phenomenon, geometric nonlinearities, squeeze-film phenomena, and environmental conditions (Barmatz and Chen, 1974; Saulson, 1990; Jazar, 2006). A more detailed calculation of m, c, and k is presented by Raskin et al., (2000). However, we accepted a constant mass, which is reasonable, and adapted a constant viscous damping which can be questionable. Furthermore, we analyzed the effects of geometric nonlinearity in stiffness and ignored all the other effects that might change it. These assumptions are valid when the system is working under steady state conditions, since after a while all environmentally related parameters will settle down at a nominal value and may be assumed constant. However, geometric related parameters must be taken into consideration even at steady state conditions.

There are some other effects such as fringing effect, van der Waals, and Casimir effects which are ignored in this analysis, since they are assumed secondary when compared with electrostatic, viscous, mid-plane stretching, and rigidity.

Introducing a set of new variables, we may transform the equation of motion to the following nondimensionalized form

$$Y'' + hY' + Y + \lambda Y^3 = \frac{1}{\left(1 - Y\right)^2}\left[\left(\alpha + \beta\right) + 2\sqrt{2\alpha\beta}\sin\left(r\tau\right) - \beta\cos\left(2r\tau\right)\right] \tag{3}$$

where,

$$\tau = \omega_n t \quad \omega_n = \sqrt{\frac{k_1}{m}} \quad Y = \frac{y}{d} \quad r = \frac{\omega}{\omega_n} \quad h = \frac{c}{\sqrt{k_1 m}} \quad k = k_1 + k_2 y^2$$

$$\alpha = \frac{\varepsilon_0 A}{2k_1 d^3} v_P^2 \quad 2\sqrt{2\alpha\beta} = \frac{\varepsilon_0 A}{k_1 d^3} v_P v_i \quad \beta = \frac{\varepsilon_0 A}{4k_1 d^3} v_i^2 \quad \lambda = \frac{k_2}{k_1} d^2. \tag{4}$$

Based on equation (3), the initial position of m in the absence of alternative and polarization voltage is at $y = 0$. However, the polarization voltage changes the static position and pulls the mass away from $y = 0$ to make an off-center vibrating system. Assuming a linear spring, $k = k_1$, the static position of the system is at the nonzero root of $Y(1 - Y)^2 = \alpha$. Under the linear assumption, the electrostatic force will overcome the restoring force at a collapse voltage

$$v_P = (d - y)\sqrt{\frac{2ky}{\varepsilon_0 A}} \tag{5}$$

which is the upper bound of polarization voltage with a safe margin. The hardening nonlinearity ($k_2 > 0$) increases the upper bound of the collapse voltage to

$$v_P = (d - y)\sqrt{\frac{2}{\varepsilon_0 A}\left(k_1 y + k_2 y^3\right)} \tag{6}$$

or in nondimensional form to

$$\alpha = \left(Y + \lambda Y^3\right)(1 - Y)^2. \tag{7}$$

The nonlinear equation (3) can be used to determine the point at which $dY/d\alpha = \infty$, yielding the exact pull-in load at $\alpha = 4/27$. Figure 2 depicts the collapse voltage as a function of displacement of the microplate for different values of the spring nonlinearities. It shows that when the polarization voltage reaches the maximum of a curve, then the electrostatic force can pull m to $y = 1$.

We may adapt an Eulerian viewpoint and remodel the microresonator so that under a fixed polarization voltage, the displacement is always measured from the working equilibrium. In this model, the electrostatic force on m would be

$$\begin{aligned} F &= \frac{\varepsilon_0 A\left(v - v_p\right)^2}{2(d - y)^2} - \frac{\varepsilon_0 A v_P^2}{2d^2} \\ &= \frac{\varepsilon_0 A}{2(d - y)^2}\left[v_P^2 + \frac{1}{2}v_i^2 + 2v_P v_i \sin(\omega t) - \frac{1}{2}v_i^2 \cos(2\omega t)\right] - \frac{\varepsilon_0 A v_P^2}{2d^2} \end{aligned} \tag{8}$$

and, the dimensionless equation of motion is

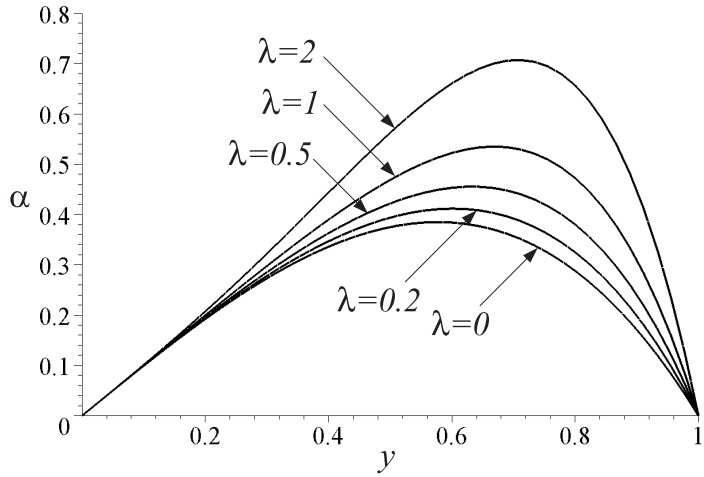

Figure 2. Possible displacement of the plate as a function of collapse load for different coefficient of nonlinear spring.

$$Y'' + hY' + Y + \lambda Y^3 = \frac{1}{(1-Y)^2}\left[(\alpha+\beta) + 2\sqrt{2\alpha\beta}\sin(r\tau) - \beta\cos(2r\tau)\right] - \alpha \quad (9)$$

so the $Y = 0$ is always the working equilibrium of the system.

Equation (9) indicates that there is a relationship between the polarization voltage and the static deflection of the supporting beam.

$$Y_s + \lambda Y_s^3 = \frac{\alpha}{(1-Y_s)^2} - \alpha. \quad (10)$$

We may also design the microresonator with no polarization voltage. In this case the electrostatic force simplifies to

$$F = \frac{\varepsilon_0 A v^2}{2(d-y)^2} = \frac{\varepsilon_0 A}{2(d-y)^2}\left[\frac{1}{2}v_i^2 - \frac{1}{2}v_i^2\cos(2\omega t)\right] \quad (11)$$

which eliminates the difference between Lagrangian and Eulerian viewpoint, because the equations of both models would be

$$Y'' + hY' + Y + \lambda Y^3 = \frac{1}{(1-Y)^2}\left[\beta - \beta\cos(2r\tau)\right]. \quad (12)$$

In this investigation, the model described by equation (9) is adapted to examine dynamics of the microresonator due to advantages of better expressing the results, compared to the traditional model in equation (3).

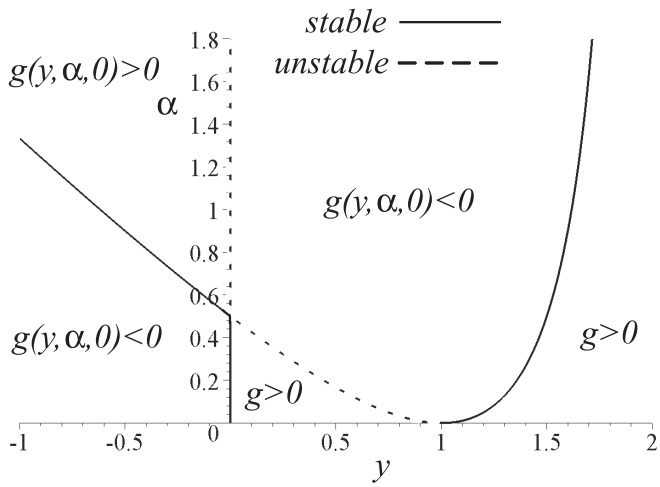

Figure 3. Position of equilibriums for the linearized MEMS as a function of α.

3. ANALYSIS

3.1. Equilibrium Position

Free vibration and equilibria of the system will be found by eliminating the excitation voltage v_i, embedded in β, and setting $Y' = Y'' = 0$.

$$Y + \lambda Y^3 - \frac{\alpha}{(1-Y)^2} + \alpha = g\,(Y, \alpha, \lambda)\,. \tag{13}$$

The solutions, $Y_i(\alpha)$ for $\lambda = 0$, represent the various steady state response branches of the system when α is a quasi-static parameter. Therefore, the equilibria of the system after ignoring the nonlinearity of stiffness would be at $Y_1 = 0$, $Y_2 = 1 - \left(\alpha + \sqrt{\alpha^2 + 4\alpha}\right)/2$, and $Y_3 = 1 - \left(\alpha - \sqrt{\alpha^2 + 4\alpha}\right)/2$, which are shown in Figure 3.

The linear stability of any particular steady state stationary solution, $y_i(\alpha)$, can be studied through linearization of the equation of motion around that solution, and investigating eigenvalues of the Jacobian J, given by $J = |\partial \mathbf{q}(Y_i, \alpha)/\partial Y|$ where $\dot{\mathbf{Y}} = \mathbf{q}(\mathbf{Y}_i, \alpha)$ is the equivalent set of first order differential equations. Stability analysis of the equilibria indicates that when $\alpha = 0$, then $Y_1 = 0$ is a center and stable, while $Y_2 = Y_3 = 1$ are vanishing coincident of an unstable source, and a stable sink (see Figure 3). Increasing α moves the unstable equilibrium Y_2 to the left and the stable equilibrium Y_3 to the right, making the stable basin around the origin narrower, and around Y_3 wider. However, $Y < 1$ indicates the limit of acceptable solution because of physical constraint. So, the third equilibrium Y_3 is out of the working space. At $\alpha = 0.5$, the collapse load appears where the equilibria Y_1 and Y_2 coincide and vanish. At this load, the system has no equilibrium within the working space, and $Y_3 = 1.5$ is the only equilibrium of the system that is stable. When $\alpha > 0.5$, the origin is no longer stable, but both Y_2 and Y_3 are stable.

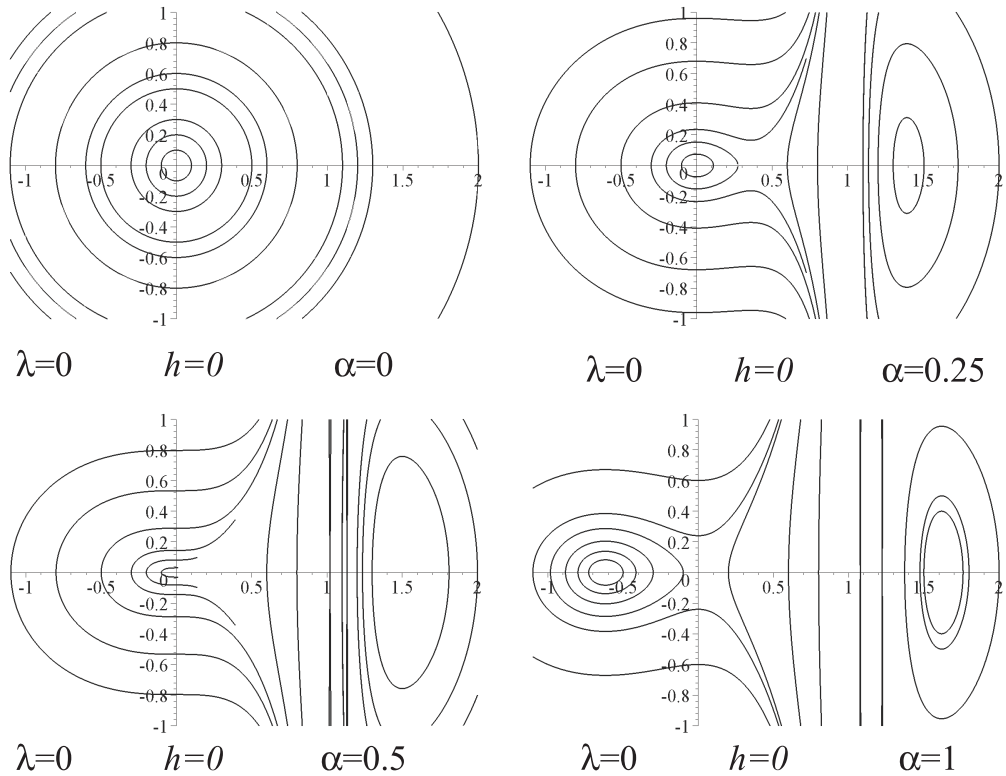

Figure 4. Phase portrait of free vibrations of the MEMS.

Because $\forall\alpha$, $J(Y_3) < 0$, this equilibrium is always stable. However, $J(Y_1) < 0$ and $J(Y_2) > 0$ for $\alpha < 0.5$ and therefore, Y_1 is a sink and Y_2 is a source. On the other hand, $J(Y_1) > 0$ and $J(Y_2) < 0$, when $\alpha > 0.5$ and therefore, Y_1 is a source and Y_2 is a sink.

Equilibria of the system and their stability behavior are illustrated in the bifurcation plot shown in Figure 3. Figure 4 depicts the phase portrait of undamped free vibration of the microresonator for different values of α. A center appears at $Y_1 = 0$ for $\alpha = 0$, then by increasing α another center appears at a position above $Y = 1$. When $\alpha = 0.5$, the center at origin disappears, and for $\alpha > 0.5$ another center appears at a negative position. The stability analysis of equilibria is equivalent to the necessary and sufficient condition that a stable path should have positive $g(Y, \alpha, 0)$ on its right hand side as shown in Figure 3 (Nayfeh and Mook, 1979).

The polarization voltage controls the position and stability of the equilibria. It is especially important for the equilibrium at origin which is supposed to be the center of vibration and becomes unstable for large values of α. However, because of nonlinearity and excitation, as soon as the resonance causes the amplitude to increase, period dependency of the amplitude causes the resonance to detune and decrease its tendency to produce large amplitude. A fact that will not be seen in linearized model. In other words, nonlinearity might help to increase the domain of stability of the system.

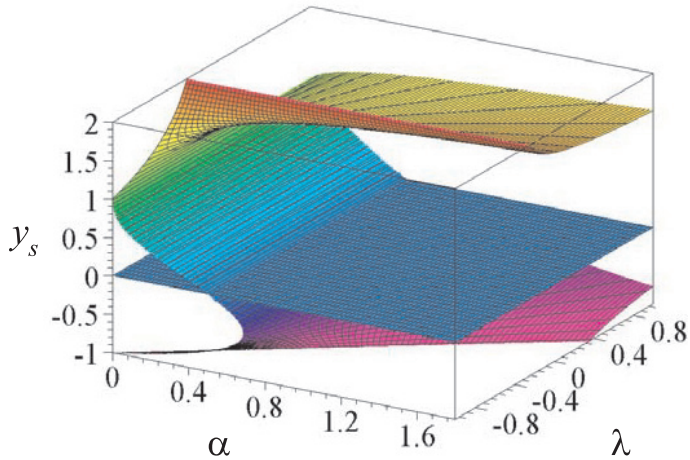

Figure 5. Equilibriua of the MEMS in parameter space.

In the absence of polarization voltage, free vibration analysis of the MEMS governs by a Duffing-type equation. Equilibria of equation (9) are given by equation (13), which implicitly defines an equilibrium surface $Y_s = u(\lambda, \alpha)$ over parametric space as shown in Figure 5. In some regions, u is a single-valued function, while in others it is a triple or pentad-valued function.

The bounding curve in parameter space indicates bifurcation. To find the bifurcation points, we locate the folds by setting $\partial^2 g/\partial Y_s^2 = 0$.

$$\frac{\partial^2 g}{\partial Y_s^2} = 6\lambda Y_s - \frac{6\alpha}{(1 - Y_s)^4} = 0. \tag{14}$$

Then, the bifurcation curves in parameter plane can be found by eliminating Y_s in equations (13) and (14), which is out of the scope of this investigation.

3.2. Linear and No Polarization Voltage

Consider a case in which $v_p = 0$. This is the simplest mathematical model of the microresonator, which has been analyzed in part by Napoli et al., (2003). Eliminating polarization voltage simplifies the governing equation to

$$Y'' + hY' + Y + \lambda Y^3 = \frac{1}{(1 - Y)^2} \left[\beta - \beta \cos(2r\tau)\right]. \tag{15}$$

Series expansion indicates that

$$\frac{1}{(1 - Y)^2} = 1 + 2Y + 3Y^2 + 4Y^3 + 5Y^4 + 6Y^5 + \mathrm{O}(Y^6). \tag{16}$$

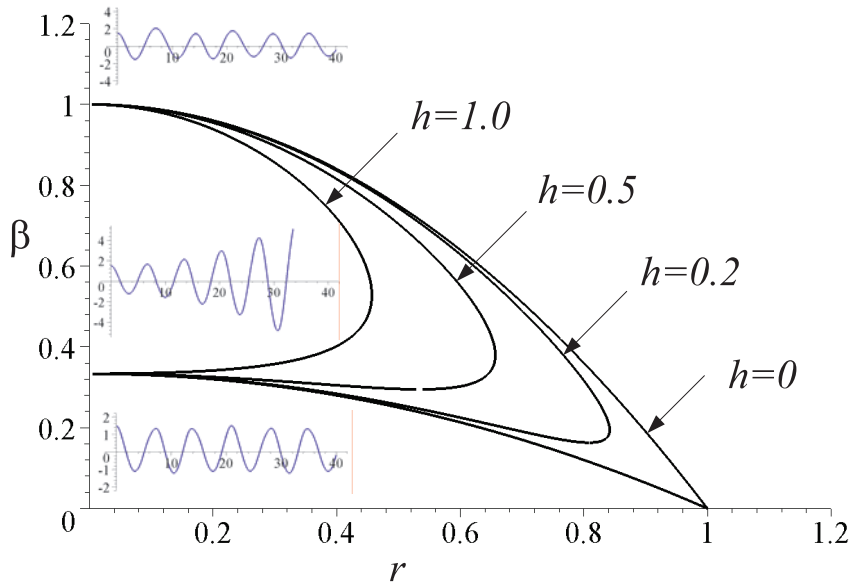

Figure 6. Transient curves and instability tongue for linear and no polarization model of the MEMS.

Assuming a very small Y and linearization of the system, converts the equation of motion to a forced Mathieu differential equation

$$Y'' + hY' + (1 - 2\beta + 2\beta\cos(2r\tau))\, Y = 2\beta\sin^2(r\tau)\,. \tag{17}$$

The transition curves in the stability plane r-β can be found by applying the multiple time scale method (Nayfeh and Mook, 1979)

$$r^2 = \frac{1}{2}\left(2 - h^2 - 4\beta \pm \sqrt{h^4 - 4h^2(1-2\beta) + 4\beta^2}\right). \tag{18}$$

Because $r^2 \in \mathbf{R}$, then h must be within the following limits

$$2 - 4\beta - 2\sqrt{3\beta^2 + 1 - 4\beta} < h^2 < 2 - 4\beta + 2\sqrt{3\beta^2 + 1 - 4\beta} \tag{19}$$

to have a transition curve. The transition curves and boundary of stability for the first instability tongue are plotted in Figure 6 for different values of h. As expected, the instability domain shrinks by increasing damping. At each excitation frequency, the domain of stability for β is

$$\frac{2}{3}\left(1 - r^2\right) - \frac{1}{3}\sqrt{\left(1 - r^2\right)^2 - 3h^2r^2} \le \beta \le \frac{2}{3}\left(1 - r^2\right) + \frac{1}{3}\sqrt{\left(1 - r^2\right)^2 - 3h^2r^2}. \tag{20}$$

Applying the Poincare-Lindstad method provides the following equations for no damping transition curves

$$\beta_1 = 1 - r^2 + \mathrm{O}(r^4) \qquad \beta_2 = \frac{1}{3} - \frac{r^2}{3} + \mathrm{O}(r^4) \tag{21}$$

which are in agreement with equation (18).

Napoli et al., (2003) have used a $200\mu m \times 50\mu m \times 2\mu m$ doped polysilicon cantilever with a gap $d = 2\mu m$, and have shown experimentally the validity of the above calculation for r near 1.

When the transient curves in parametric plane β-r are determined by either multiple scale, averaging or Poincare-Lindstad methods, the stable and unstable regions can be determined by investigating time response of a picked point. Selecting $(r, \beta) = (0.2, 0.1)$, $(0.9, 0.1)$, and $(1.2, 0.1)$ in the three regions divided by curves of equation (21) for $h = 0$, generates the time responses shown in Figure 6.

3.3. Nonlinear and No Polarization Voltage

When the amplitude of vibration increases, the linear approximation of the model is no longer appropriate. Hence, we have to adopt a nonlinear approximation. The nonlinear model of the system up to $O(y^2)$ is

$$y'' + hy' + (1 - 2\beta + 2\beta\cos(2r\tau))\, y - 3\,(\beta - \beta\cos(2r\tau))\, y^2 = u(\tau), \tag{22}$$

and up to $O(y^3)$ is

$$\begin{aligned} & y'' + hy' + (1 - 2\beta + 2\beta\cos(2r\tau))\, y - 3\,(\beta - \beta\cos(2r\tau))\, y^2 \\ + \quad & (\lambda - 4\beta + 4\beta\cos(2r\tau))\, y^3 \;=\; u(\tau). \end{aligned} \tag{23}$$

However, the following nonlinear equation must be analyzed if no simplification is made.

$$y'' + hy' + y + \lambda y^3 = \frac{1}{(1-y)^2}\left[\beta - \beta\cos(2r\tau)\right]. \tag{24}$$

Equation (22) indicates a forced nonlinear parametric equation. It can be shown that applying multiple time scale method provides the same transition curves as presented in (18). In addition, the Lindstad-Poincare method generates the same transition curves (21). So, based on perturbation analysis, the stability diagrams for systems (17) and (22) are identical.

Equation (23) also indicates a forced nonlinear parametric equation, however it is more accurate than (22) when amplitude of oscillation is higher and nonlinearity of spring is included. The cubic term of (22) provides a possible frequency response. Using multiple time scale method and searching for a steady state response as $y = Y(t)\sin(rt + \varphi(t))$, the following equation describing the frequency response of the MEMS will be obtained.

Table 1. Nominal values of the dynamic parameters of the MEMS.

m	1×10^{-11} kg
c	1×10^{-8} Ns/m
k	1 N/m
d	2.0 μm
A	200×50 μm

$$\begin{aligned} & \left[(3\lambda - 4\beta)\, Y^2 - 4\left(r^2 + \beta - 1\right)\right]^2 \left(Y^2 + 1\right)^2 \\ + \quad & 16\beta\left(1 + 2Y^2\right)\left[(3\lambda - 4\beta)\, Y^2 - 4\left(r^2 + \beta - 1\right)\right]\left(Y^2 + 1\right)^2 \\ + \quad & 64h^2 r^2\left(1 + 2Y^2\right) \;=\; 0. \end{aligned} \tag{25}$$

In what follows, a set of nominal values of a sample micrcantilever resonator, indicated in Table 1, are adopted to analyze the dynamic behavior of the MEMS, although because of dimensionless forms of the equations, any other microcantilever resonator can be analyzed as well (Kaajakari et al., 2001; Kanda et al., 2000; Yang et al., 2002; Khaled et al., 2003).

Frequency response of the system for different values of nonlinear spring and damping rates, are plotted in Figures 7(a) to 7(f).

When there is no damping ($h = 0$), frequency response is obtained by two curves starting from

$$r = 1 - 2\beta \pm \beta \tag{26}$$

however, the curvature of these curves is a function of the spring nonlinearity λ. Analysis of equation (25) clarifies how the frequency response of the model (23) is complicated. Setting $\beta = 0.1$, and starting from a large value of λ, say $\lambda = 1.0$, the frequency response would be analogous to Figure 7(a). Stability analysis of this kind of frequency response is presented in a some references such as (Minorsky, 1949; Nayfeh and Mook, 1979). It can found by perturbing the steady state periodic solution $y = Y \sin(rt + \varphi(t))$ by adding a small perturbation function, $p = y + \varepsilon(t)$, and considering the linearized equation of motion. In a frequency sweep experiment, the left branch started from $r = 1 - h^2/2 - 2\beta - \sqrt{h^4 + 4h^2(2\beta - 1) + 4\beta^2}$ will be followed by the system up to the frequency $r = 1 - h^2/2 - 2\beta + \sqrt{h^4 + 4h^2(2\beta - 1) + 4\beta^2}$ where it jumps down to the lower curve. The stability analysis also indicates when one branch of frequency response has shadow on the other one; the lower one is the stable branch.

For $\lambda > 2/3$ no steady state motion is possible at any frequencies less than $r = 1 - \beta = 0.9$, as shown in Figure 7(b). For $2/15 < \lambda < 2/3$, the frequency response of the system is shown in Figure 7(c). When $\lambda < 2/15$, no steady state motion is possible at any frequencies greater than $r = 1 - \beta = 0.9$, as shown in Figure 7(d). By reducing λ, a frequency response shown in Figure 7(e) will be achieved. Frequency response of the system is multi-valued, when $\lambda < 2/15$, or $\lambda > 2/3$.

When the nonlinearity is dominant and the approximated equation (23) is not acceptable as a substitute for (24), the exact model (23) must be analyzed. Assuming a harmonic solution in the form $y = Y(t)\sin(rt + \varphi(t))$, the following equation describing the frequency

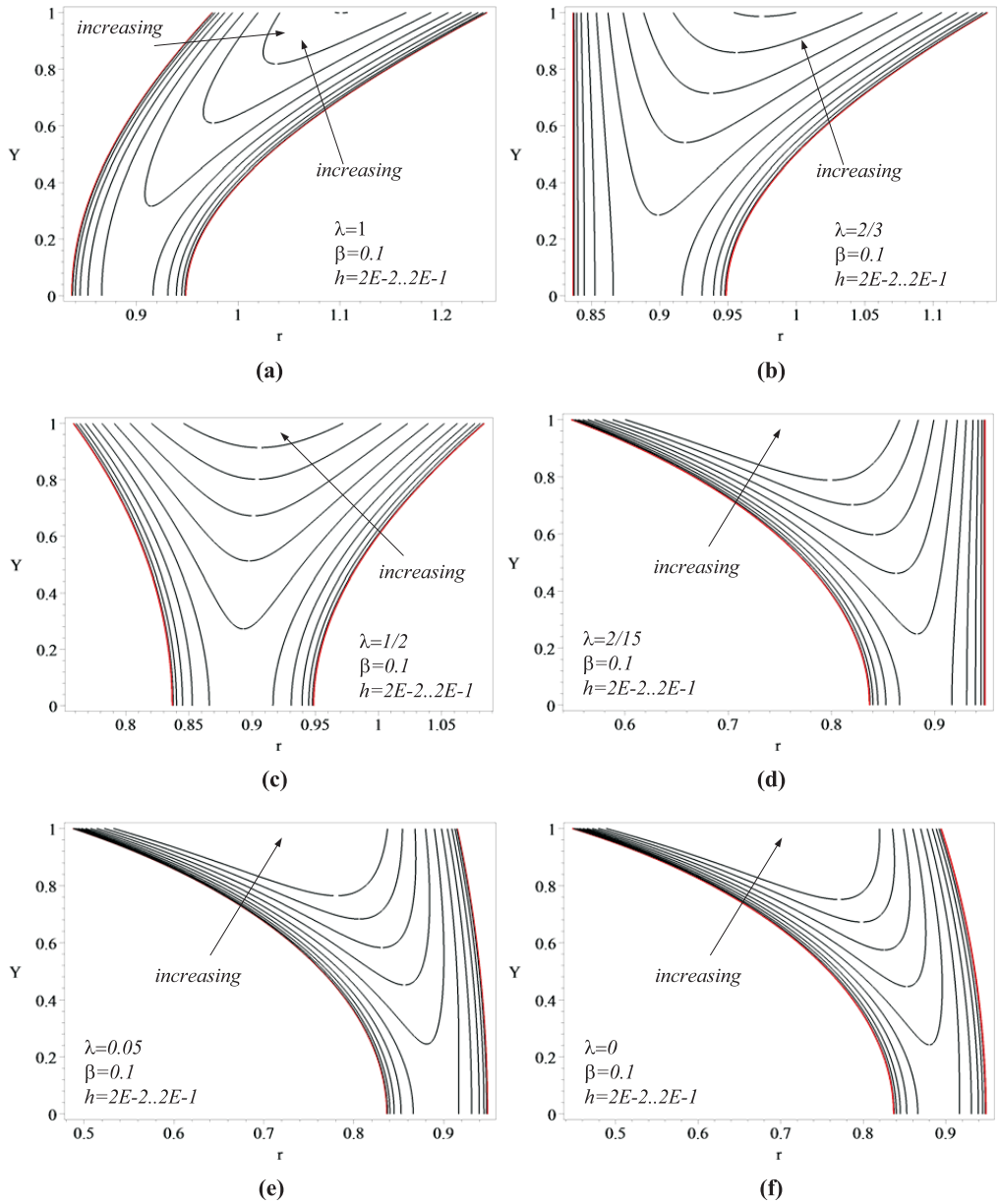

Figure 7. Frequency response of the MEMS act upon Equation (23), for a set of parameters.

response of the nonpolarized model of the MEMS will be obtained by applying a multiple scale method.

$$Z_1^2 + \beta Z_1 + 2h^2 r^2 = 0 \tag{27}$$

where,

$$Z_1 = 4 + 4\beta + 3\lambda Y^2 - 4r^2. \tag{28}$$

Up to this point, the frequency response (27) is the best equation that describes the steady state behavior of the system. It will be shown, by a parametric analysis, how the frequency response of the model (26) differs from the approximate solution (24).

Analysis of equation (27) indicates that $|r| \leq \beta/h$ is the boundary for excitation frequency to have a nontrivial steady state response. It also indicates when $\lambda = 0$, the amplitude goes to infinity and the frequency response reduces to the following two vertical lines.

$$r = -\frac{h^2}{2} + 2\beta + 1 \pm \frac{\sqrt{h^4 - 4h^2 - 8h^2\beta + 4\beta^2}}{2}. \tag{29}$$

The two branches of frequency response reach each other at the peak amplitude, which would be

$$Y_{Max} = \frac{\sqrt{6\lambda\left(h^2 - 4\beta - 2\right)}}{3\lambda}. \tag{30}$$

Figure 8(a) depicts the frequency response of the MEMS for a highly nonlinear spring rate, and shows the effect of damping rate on steady state response. As expected, increasing the value of damping rate decreases the amplitude. The maximum acceptable damping is $h = \beta/r_0$, where r_0 is the average of the two branches given in (29). Figure 8(b) depicts the effect of decreasing of spring nonlinearity. Some significant differences can be seen when Figures 7 and 8 are compared. First, the two branches of the frequency response of model (23) converge as long as there is some damping in the systems. Second, its frequency response curves bend to positive frequencies regardless of the value of nonlinear spring rate. Third, the steady state response curves start from $r > 1$ instead of $r < 1$.

The effect of excitation amplitude, β, is shown in Figure 8(c). Peak amplitude increases and frequency response curves shift to higher frequencies when β increases. Figure 8(d) represents that increasing λ, bends the curves of frequency response. equation (30) also proves that the peak value of amplitude reduces by increasing λ.

3.4. Linear with Polarization Voltage

Dynamics behavior of the MEMS is more interesting when a polarization voltage is present. Assuming polarization voltage is less than the collapse voltage, and $y \ll 1$, the governing equation of the MEMS is

$$\begin{aligned} & y'' + hy' + \left(1 - 2\beta - 2\alpha + 2\beta\cos\left(2r\tau\right) - 4\sqrt{2\alpha\beta}\sin\left(2r\tau\right)\right) y \\ = \;& 2\beta\sin^2\left(r\tau\right) + 2\sqrt{2\alpha\beta}\sin\left(r\tau\right). \end{aligned} \tag{31}$$

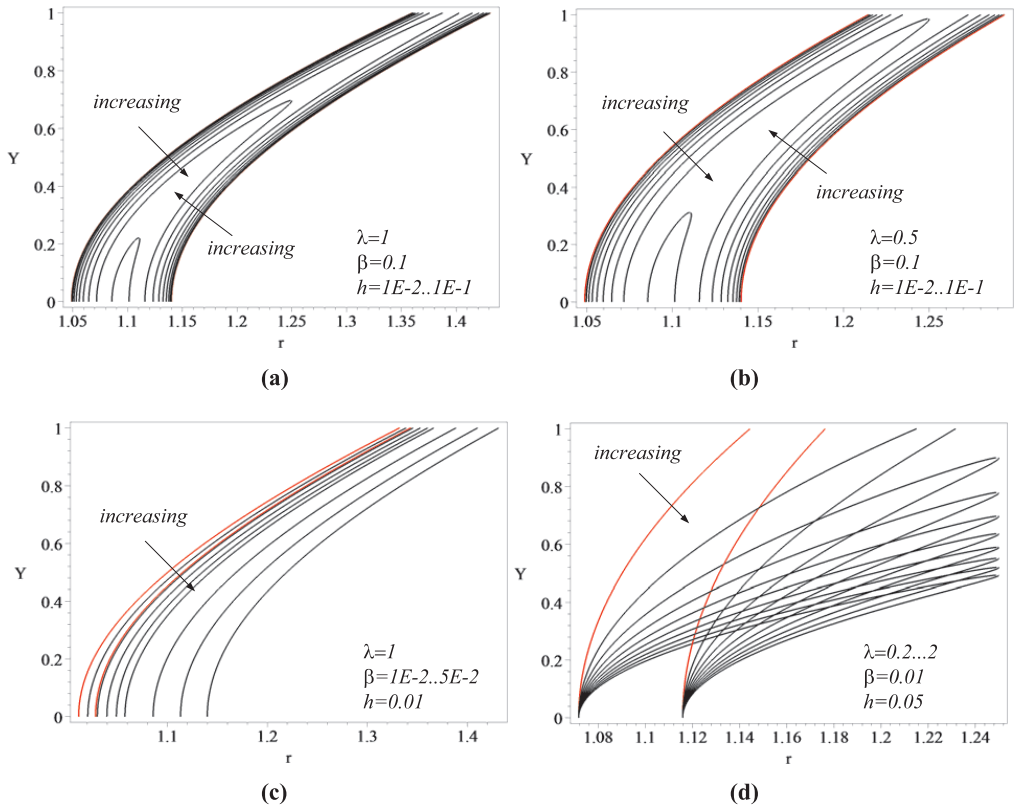

Figure 8. Frequency response of the MEMS act upon Equation (24), for a set of parameters.

It can be shown that applying averaging method provides the following frequency response.

$$4\beta^2 Y^4 r^4 + 4\beta^2 Y^4 r^2 \left(4\left(\beta+\alpha\right)+h^2-2\right) + 2\beta^2 Y^4 \left(1-\beta-2\alpha\right)\left(1-3\beta-2\alpha\right)$$
$$- \quad 16\beta^3 Y^2 \left[\sqrt{\alpha\left(\alpha-r^2Y^2\right)+\alpha\left(1-\beta-2\alpha\right)Y^2}-\alpha\right] \;=\; 0. \tag{32}$$

A plot of equation (32), shown in Figure 9(a), indicates that by introduction of polarization voltage the system vibrates as a well-behaved resonator. Since nonlinearities are ignored, there would be no jump in steady state response, and there is no difference between positive and negative frequency sweeps. The frequency response is stable in this case.

The effect of varying parameters β and α are plotted in Figures 9(b) and 9(c), respectively. As seen in these Figures the amplitude of response increases by increasing both β, and α. Although equation (32) is not as simple as the frequency response of a linear mass-spring-damper system, it can still be used for RMS optimization, if reduction in the level of absolute acceleration and relative displacement are the parameters of interest (Jazar et al.,

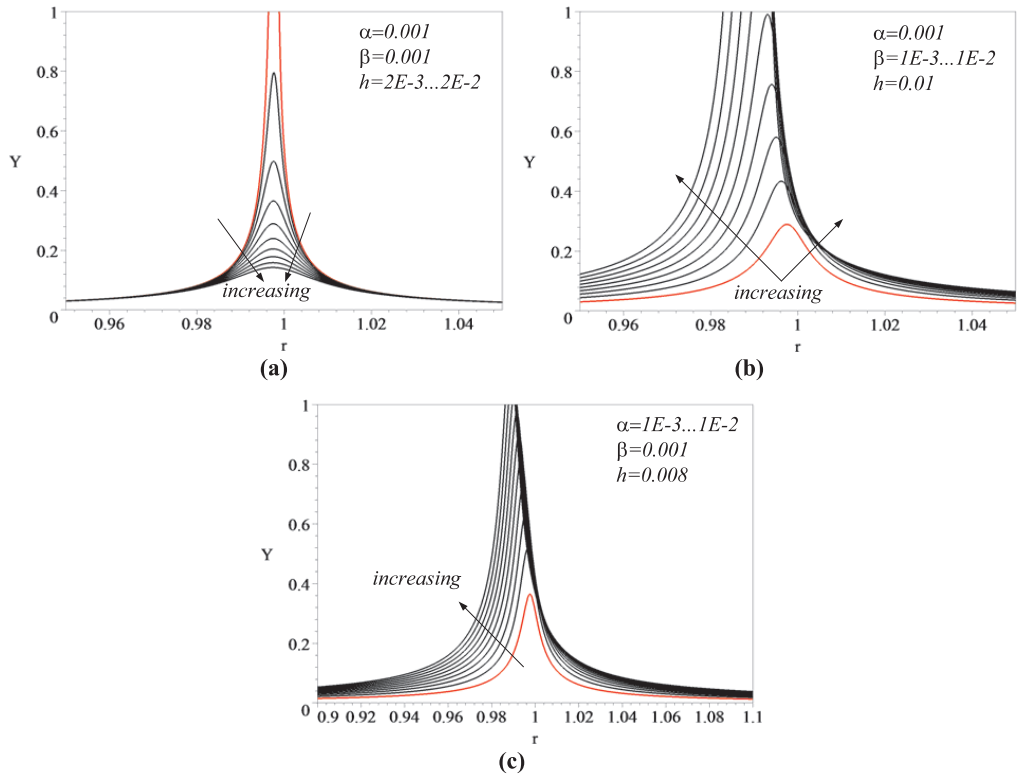

Figure 9. Frequency response of the linearized microresonator with polarization.

2003). Applying the RMS optimization might be justified, because reduction in the relative displacement reduces the effect of nonlinearity and makes the linear model reasonable.

3.5. Nonlinear with Polarization Voltage

Complete analysis of the MEMS is performed when the nonlinearity is included in the polarized model. If there exist a small nonlinearity up to $O(y^2)$, the equation of motion becomes

$$\begin{aligned} & y'' + hy' + \left(1 - 2\beta - 2\alpha + 2\beta\cos(2r\tau) - 4\sqrt{2\alpha\beta}\sin(r\tau)\right) y \\ - \; & 3\left(\beta + \alpha - \beta\cos(2r\tau) + 2\sqrt{2\alpha\beta}\sin(r\tau)\right) y^2 \\ = \; & 2\beta\sin^2(r\tau) + 2\sqrt{2\alpha\beta}\sin(r\tau)\,. \end{aligned} \tag{33}$$

By increasing the effect of nonlinearity and including $O(y^3)$, the equation of motion would be

$$
\begin{aligned}
& y'' + hy' + \left(\lambda - 4\beta - 4\alpha + 8\beta\cos(2r\tau) - 8\sqrt{2\alpha\beta}\sin(r\tau)\right) y^3 \\
- \; & 3\left(\beta + \alpha - \beta\cos(2r\tau) + 2\sqrt{2\alpha\beta}\sin(r\tau)\right) y^2 \\
+ \; & \left(1 - 2\beta - 2\alpha + 2\beta\cos(2r\tau) - 4\sqrt{2\alpha\beta}\sin(r\tau)\right) y \\
= \; & 2\beta\sin^2(r\tau) + 2\sqrt{2\alpha\beta}\sin(r\tau)\,. \qquad (34)
\end{aligned}
$$

In general, when no approximation is applied on $1/(1-y)^2$, the equation of motion would be

$$
y'' + hy' + y + \lambda y^3 = \frac{1}{(1-y)^2}\left[(\alpha+\beta) + 2\sqrt{2\alpha\beta}\sin(r\tau) - \beta\cos(2r\tau)\right] - \alpha. \qquad (35)
$$

Employing averaging method determines the steady state frequency response of equation (33) to be

$$
Z_2 Z_3 - 64Y^2\beta^2 Z_2 + 1024Y^4\beta^2 h^2 r^2 = 0 \qquad (36)
$$

where

$$
\begin{aligned}
Z_2 &= \left(\left(3Y^2 - 4\right)\sqrt{2\alpha\beta} - Z_4\right)^2 && (37)\\
Z_3 &= \left(\left(9Y^2 - 4\right)\sqrt{2\alpha\beta} + Z_4\right)^2 && (38)\\
Z_4 &= \sqrt{162Y^4\alpha\beta + 32Y^2\beta\left(1 - r^2 - \beta + 2.5\alpha\right) + 32\alpha\beta}, && (39)
\end{aligned}
$$

and frequency response of equation (34) using the same method is

$$
Z_5 Z_6 - 256\beta^2 Y\left(2Y^2+1\right)^2 Z_5 + 4096Y^3 h^2 r^2 \beta^2\left(2Y^2+1\right)^4 = 0 \qquad (40)
$$

where

$$
\begin{aligned}
Z_5 &= \left(\left(3Y^2 - 9Y + 4\right)\sqrt{2\alpha\beta} + \left(Y^2+1\right) Z_7\right)^2 && (41)\\
Z_6 &= \left(\left(-18Y^2 - 8\right)\sqrt{2\alpha\beta} + 2Z_7\right)^2 && (42)\\
Z_7 &= \sqrt{2\beta}\sqrt{\begin{pmatrix} 8Y^6(3\lambda - 4\beta - 12\alpha) + Y^4\left(32 - 31\alpha - 32r^2 - 48\beta + 12\lambda\right) \\ +16Y^2\left(1 - r^2 - \beta + 2.5\alpha\right) + 16\alpha \end{pmatrix}}. && (43)
\end{aligned}
$$

Figure 10 illustrates the frequency response of equation (32) and Figure 11 depicts the response of (39).

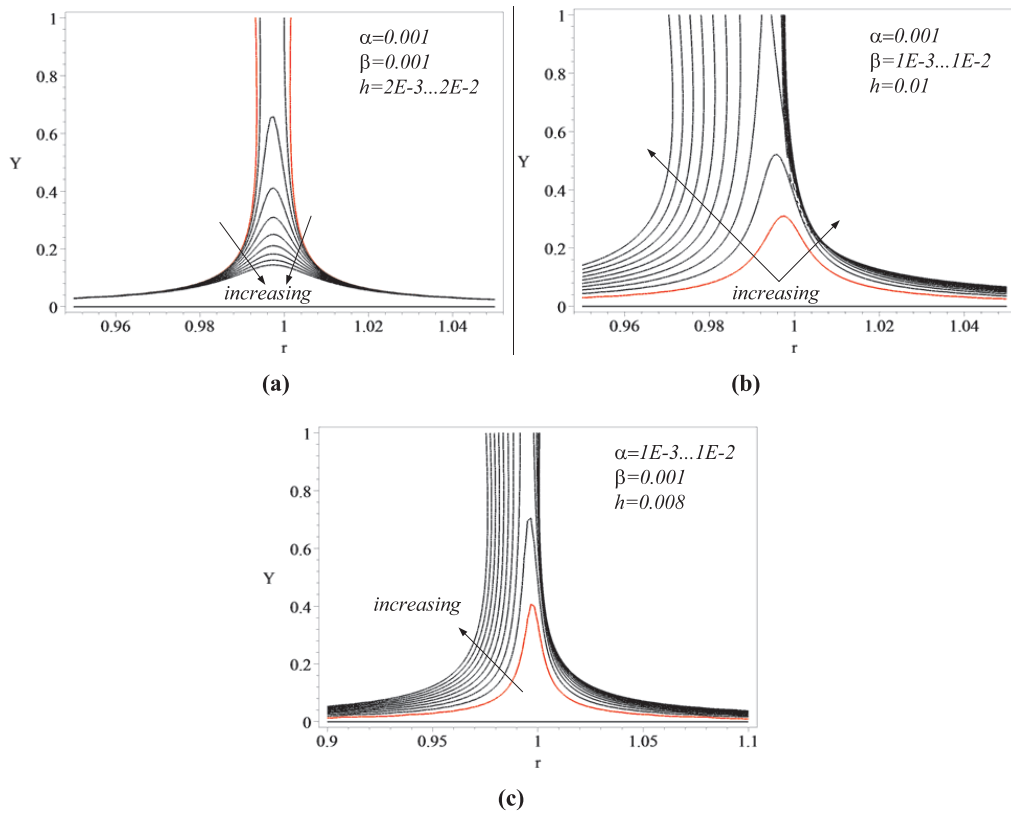

Figure 10. Frequency response of the $O(y^2)$ nonlinear microresonator with polarization.

Comparing Figures 9 and 10 indicates that the resonance domain will be widening by including a slight nonlinearity. In addition, the peak amplitude of the system is higher for Figure 10. Therefore, including second degree nonlinearities provides a more sensitive system with a more probability of impact to the fixed electrode.

Including third degree nonlinearities complicates the dynamic of the resonator, by introducing jump phenomenon and possible frequency island (Jazar and Golnaraghi, 2002). Figures 11(a) to 11(c) show the steady state behavior for a linear stiffness ($\lambda = 0$), while Figures 11(d) to 11(f) include the stiffness nonlinearity. The nonlinearity of the electrostatic force bends the frequency responses to lower frequencies; however, the stiffness nonlinearity has opposite effect and reduces the bending effect of electrostatic nonlinearity. Therefore, the possibility of jump can be reduced by designating the stiffness nonlinear rate.

After providing the frequency response of equations (36) and (40) the frequency response of the fully nonlinear model (35) will be investigated. Assuming a harmonic solution at steady state condition, $y = Y(t)\sin(rt + \varphi(t))$, and applying averaging method, the following frequency response will be obtained

$$Z_8 Z_9 - 64\beta^2 Y^2 Z_8 + 256 Y^4 h^2 r^2 \beta^2 = 0 \tag{44}$$

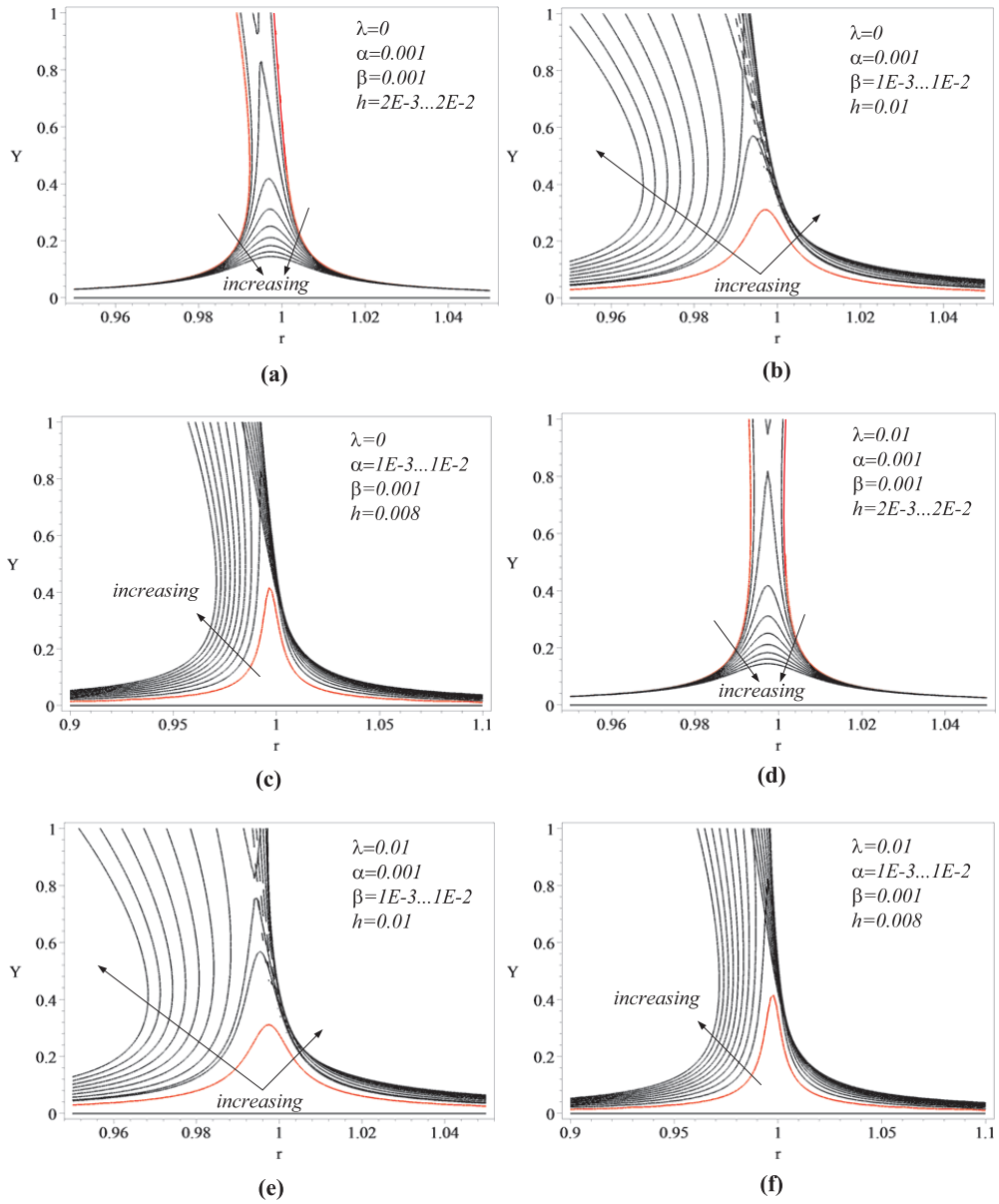

Figure 11. Frequency response of the $O(y^3)$ nonlinear microresonator with polarization.

where

$$Z_8 = \left(2\sqrt{2\alpha\beta} + Z_{10}\right)^2 \tag{45}$$

$$Z_9 = \left(-4\sqrt{2\alpha\beta} + 2Z_{10}\right)^2 \tag{46}$$

$$Z_{10} = \sqrt{6Y^4\beta\lambda + 8Y^2\beta\left(1 - r^2 - \beta - 2\alpha\right) + 8\alpha\beta}. \tag{47}$$

Although the complete model of the MEMS dynamic is described by a highly nonlinear ODE with parametrically and externally excitations, plot of equation (44) illustrates that frequency responses of the system looks like the response of an externally excited nonlinear system, say Duffing equation. Jump phenomenon is one of the most important characteristics of the system, indicating that the response of the system, depending on history of the excitation frequency, are not equal around resonance.

In order to visualize the frequency response of the system, Figures 12(a) and (d) depict the effect of damping rate on the frequency response of the system for a set of parameters. Effect of β and α are also shown in Figures 12(b), (c), (e) and (f). Figures 12(d)–(f) examine a positive λ. In order to compare the effect of nonlinearity of the spring in the frequency response of the MEMS, two sets of plots have been provided for linear spring, i.e., $\lambda = 0$, and hardening spring, $\lambda > 0$.

4. COMMENTS

In a series of reports available in archived literature, this system is modeled by the following equation,

$$y'' + cy' + (a - 2q\cos 2\tau)\, y = qd\cos^2 t$$

where,

$$a = \frac{k}{m\omega^2} - \frac{\varepsilon_0 A}{2km\omega^2 d^3}v_i^2 \quad q = \frac{\varepsilon_0 A}{4km\omega^2 d^3}v_i^2.$$

In order to include nonlinearity, few investigators have added a cubic stiffness to the restoring force element, and adopted one of the following equations as the governing equation of motion.

$$y'' + cy' + (a - 2q\cos 2\tau)\, y - by^3 = qd\cos^2 t$$

$$y'' + cy' + (a_1 - 2q_1\cos 2\tau)\, y - (a_2 - 2q_2\cos 2\tau)\, y^3 = 0$$

$$y'' + cy' + (a - 2q\cos\tau - 2q\cos 2\tau)\, y - by^3 = qd\cos^2 t$$

$$y'' + cy' + (a - 2q\cos\tau - 2q\cos 2\tau)\, y - by^3 = qd\cos^2 t + qd\cos t.$$

Accepting a cubic nonlinearity for stiffness of the supporting beam, and not including the first four terms of Taylor expansion of the electric force,

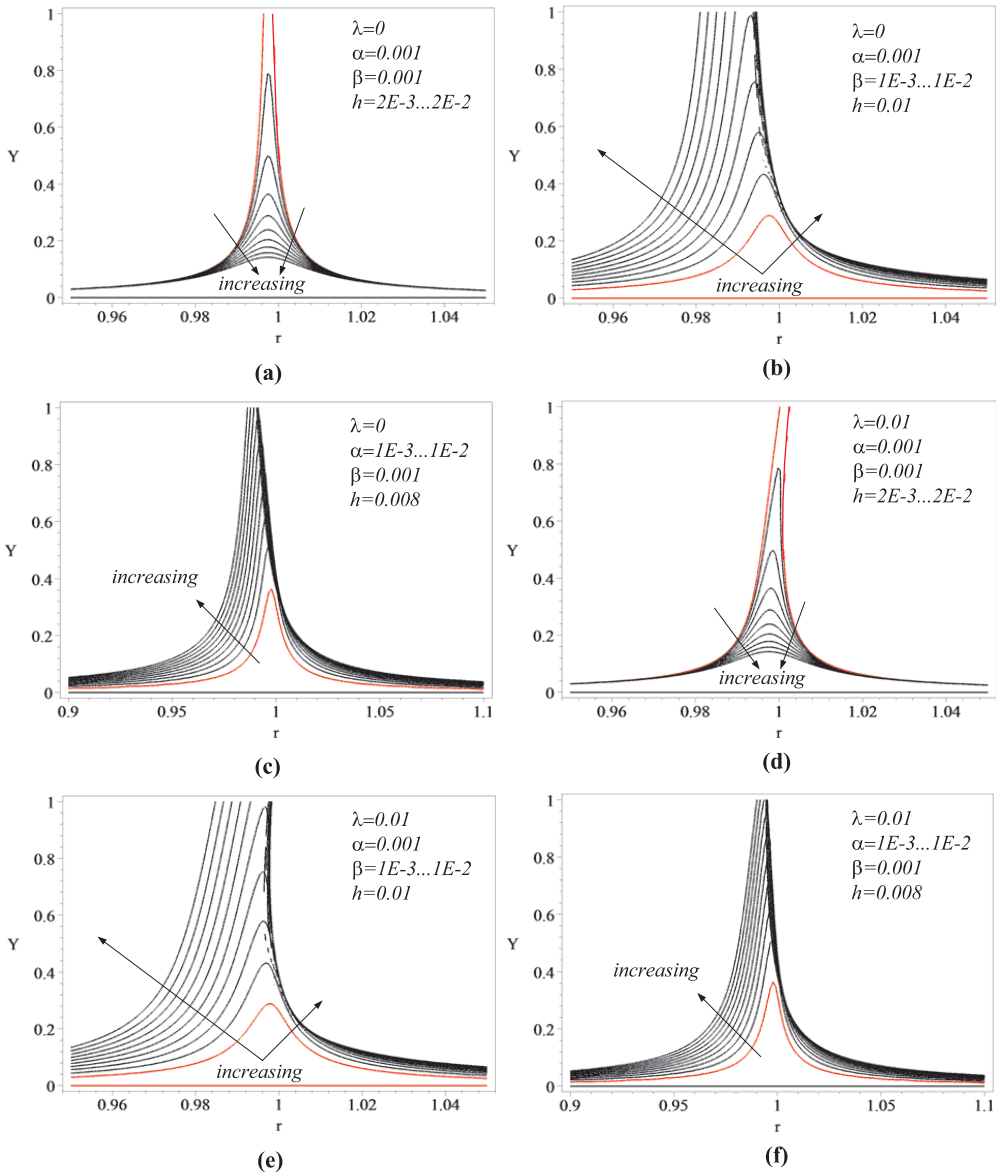

Figure 12. Frequency response of the nonlinear microresonator with polarization.

$$\frac{1}{(1-y)^2} = 1 + 2y + 3y^2 + 4y^3 + 5y^4 + 6y^5 + \mathrm{O}(y^6)$$

is not a reasonable simplification. Adopting a nonlinear equation for electric force is much more important than including a cubic stiffness, since a linear spring can be built, but a linear electric force is impossible to be made.

5. CONCLUSION

A comprehensive model of an electric actuated microcantilever MEMS has been developed, and it is shown that its dynamic behavior is governed by a highly nonlinear ODE with parametrical and external excitations. Using the complete equation of motion, equilibria, their stability, and collapsing voltage have been investigated. It is shown that the polarization voltage is the most important physical parameters in controlling the stability of equilibria and their bifurcation.

At first, the polarization voltage was set to zero. After a simplification by linearizing the restoring and electric forces, a harmonic externally excited Mathieu equation was used to investigate the dynamics of the MEMS. The analytic result based on perturbation methods was derived and compared with the stability diagram to indicate the boundary of acceptability of perturbation result. By increasing the effect of amplitude, the second degree term in the series expansion of the electric force has been included. The resulting equation showed no frequency response, and applying perturbation methods produced no new stability diagram. Consideration of higher amplitudes included the third degree term of electric force expansion and the cubic term of restoring force element. Appearance of a cubic term causes a frequency response that has been found using perturbation methods. The frequency response of the system was not similar to the frequency response of a familiar vibrating system, and a sensitivity analysis designated the dominant effect of the cubic spring rate in frequency response of the system.

Dynamic behavior of the MEMS is radically different when a polarization voltage exists. Polarized MEMS shows a familiar and well-behaved frequency response, even for a linearized approximation. The frequency response equation has been derived by applying perturbation methods when the restoring stiffness and electric force were substituted by their linear equivalents. The effects of varying polarization voltage, input voltage, and damping of the system embedded in $\alpha = \varepsilon_0 A v_P^2/2k_1 d^3$, $\beta = \varepsilon_0 A v_i^2/4k_1 d^3$, and $h = c/\sqrt{k_1 m}$ have been illustrated and analyzed. By considering higher amplitudes and including second, and third degree terms, two new approximated models of the system were presented. Frequency responses of the models were found by applying averaging and multiple scale methods. The frequency response equations have been reported.

The almost exact model of the MEMS, including polarization voltage, nonlinear spring rate, and one over square electrostatic force law, has been investigated at steady state conditions. Applying perturbation method, an equation has been developed to describe the frequency response of the MEMS. The steady state response of the system is governed by four parameters, $\alpha = \varepsilon_0 A v_P^2/2k_1 d^3$, $\beta = \varepsilon_0 A v_i^2/4k_1 d^3$, $h = c/\sqrt{k_1 m}$, and $\lambda = d^2 k_2/k_1$, in addition to the excitation frequency $r = \omega/\omega_n$. The frequency response of this model has been analyzed extensively to illustrate the effect of individual parameters. In order to provide a general investigation, soft and hard springs as well as linear spring were also analyzed. The steady state response of the system has shown interesting behavior for negative λ. Nonlinear characteristics of the model causes the frequency response to show a jump phenomenon for a range of parameters. Frequency response analysis is the first step in design of the system, which must be followed up by optimization. Another independent study is needed to undertake the optimization problem, which is out of the scope of this investigation. Optimization of the system, for minimum acceleration with respect to relative displacement is a suspension

optimization problem. Appearance of a jump in frequency response makes the optimization problem complicated. Jump avoidance conditions must be derived to restrict the acceptable domain of physical parameters. Frequency response of the system represents a triple valued function for some range of parameters. They also appear in two separate branches, which make a double jump for some range of parameters.

REFERENCES

Barmatz, M. and Chen H. S., 1974, "Young's modulus and friction in metallic glass alloys from 1.5 to 300 K", *Journal of Physical Review B* **9(10)**, 4073–4083.

Hsu, T. R., 2002, *MEMS & Microsystems Design and Manufacture*, MGraw Hill, New York.

Jazar, G. N. and Golnaraghi, M. F., 2002, "Nonlinear modeling, experimental verification, and theoretical analysis of a hydraulic engine mount," *Journal of Vibration and Control* **8(1)**, 87–116.

Jazar, G. N., Narimani, A., Golnaraghi, M. F., and Swanson, D. A., 2003, "Practical frequency and time optimal design of passive linear vibration isolation mounts," *Journal of Vehicle System Dynamics* **39(6)**, 437–466.

Jazar, G. N. 2006, "Mathematical modeling and simulation of thermoelastic effects in flexural microcantilever resonators dynamics," *Journal of Vibration and Control* **12(2)**, 139–163.

Kaajakari, V., Mattila, T., Kiihamaki, J., Kattelus, H., Oja, A., and Seppa, H., 2003, "Nonlinearities in single-crystal silicon micromechanical resonators," in *Proceedings of the 12th International Conference on Transducers, Solid-State Sensors, Actuators and Microsystems*, Boston, MA, June 8–12, pp. 1574–1577.

Kanda, T., Morita, T., Kurosawa, M. K., and Higuchi, T., 2000, "A flat type touch probe sensor using PZT thin film vibrator," *Sensors and Actuators* **83**, 67–75.

Khaled, A. R. A., Vafai, K., Yang, M., Zhang, X., and Ozkan, C. S., 2003, "Analysis, control and augmentation of microcantilever deflections in bio-sensing systems," *Sensors and Actuators B* **94**, 103–105.

Minorsky, N., 1949, *Nonlinear Oscillations*, van Nostrand, NY Princeton, NJ.

Napoli, M., Baskaran, R., Turner, K., and Bamieh, B., 2003, "Understanding mechanical domain parametric resonance in microcantilevers," in *IEEE The Sixteenth Annual International Conference on Micro Electro Mechanical Systems MEMS-03*, Kyoto, Japan, January 19–23 *2003*.

Nayfeh, A. H. and Mook, D. T., 1979, *Nonlinear Oscillations,* Wiley, New York.

Nayfeh, A. H. and Younis, M. I., 2004, "A new approach to the modeling and simulation of flexible microstructures under the effect of squeeze-film damping," *Journal of Micromechanics and Microengineering*, **14**, 170–181.

Nguyen, C. T. C., 1995, "Micromechanical resonators for oscillators and filters," in *Proceedings of IEEE International Ultrasonic Symposium*, Seattle, WA, pp. 489–499, November 7–10.

Raskin, J. P., Brown, A. R., Khuri-Yakub, B. T., and Rebeiz, G. M., 2000, "A novel parametric effect MEMS amplifier," *Journal of Microelectromechanical Systems* **9(4)**, 528–537.

Saulson, P. R., 1990, "Thermal noise in mechanical experiments," *Physical Review D* **42(8)**, 2437–2445.

Sigmund, O., 2001, "Design of multiphysics actuators using topology optimization – part I: One-material structure," *Computational Methods Applied Mechanical Engineering* **190**, 6577–6604.

Wang, K., Wong, A. C., and Nguyen, C. T., 2000, "VHF free-free beam high-Q micromechanical resonators," *Journal of Microelectromechanical Systems* **9**, 347–360.

Yang, J. L., Ono, T., and Esashi, M., 2002, "Energy dissipation in submicrometer thick single crystal silicon cantilevers," *Journal of Microelectromechanical Systems* **11**, 775–783.

Younis, M., I., Abdel-Rahman, E. M., and Nayfeh, A. H., 2003, "A reduced-order model for electrically actuated microbeam-based MEMS," *Journal of Microelectromechanical Systems* **12(5)**, 672–680.

Younis, M. I. and Nayfeh, A. H., 2003, "A study of the nonlinear response of a resonant microbeam to electric actuation," *Nonlinear Dynamics* **31**, 91–117.

Younis, M. I., 2004, "Modeling and Simulation of Microelectromechanical Systems in Multi-Physics Fields," Ph.D. thesis, *Virginia Polytechnic Institute and State University,* Blacksburg, VA.